Food & Function

ROYAL SOCIETY OF CHEMISTRY

PAPER

View Article Online
View Journal

Cite this: DOI: 10.1039/d6fo00704j

Cyanidin and delphinidin inhibit transglutaminase 2 and mitigate inflammatory effects of IFN-γ and TNF-α by molecular interaction

Andrea Diers, *[a,b] Silvia Rudloff,[a,b] Heike Hausmann,[d] Anika E. Wagner [b,c] and Sebastian Stricker[a]

Enzymatic modification of gliadin peptides by calcium-dependent transglutaminase 2 (TG2) plays a central role in the pathogenesis of celiac disease (CD) and is considered a potential therapeutic target. Recently, anthocyanins (ACN) such as cyanidin-3-glucoside (C3G) and delphinidin-3-glucoside (D3G) have gained attention in CD research for their anti-inflammatory, antioxidant and gliadin-binding properties. This study examined whether C3G and D3G modulate TG2 activity and cytokine-induced inflammation in human intestinal cells. TG2 activity was analyzed using gliadin substrates and TG2 expression was assessed after IFN-γ and TNF-α stimulation. Cell viability after ACN, IFN-γ and TNF-α incubation was tested with a resazurin-based fluorometric assay. Docking and STD-NMR experiments were conducted to explore the molecular interactions involved. D3G significantly reduced TG2-mediated crosslinking of gliadin and C3G of 5-biotinamidopentylamine as a synthetic substrate of TG2. STD-NMR and *in silico* docking experiments revealed a molecular interaction of ACN with calcium binding sites of TG2 which are essential for its enzymatic function. In addition, C3G and D3G improved cell viability under IFN-γ and TNF-α exposure and D3G reduced upregulation of TG2 mRNA under IFN-γ stimulation. Here, *in silico* docking experiments suggested that both ACN may interact with the assembly of cytokines and their corresponding cellular receptors. In conclusion, our data indicates that C3G and D3G reduce TG2-activity and mitigate cytokine-mediated inflammatory effects by a direct molecular interaction. This supports their potential as natural modulators of TG2 in the context of CD.

Received 12th February 2026,
Accepted 5th May 2026

DOI: 10.1039/d6fo00704j

rsc.li/food-function

Introduction

Celiac disease (CD) represents a chronic, systemic autoimmune disorder, triggered by the ingestion of gliadin and related prolamines in genetically predisposed (HLA-DQ2/DQ8 genotype) individuals.[1] The disease is associated with diverse intestinal symptoms such as diarrhea or abdominal bloating and extraintestinal symptoms, *e.g.*, failure to thrive or anemia as well as an increased mortality.[2,3] On a molecular basis, gluten, the main protein fraction in wheat, rye and barley, is only partially digested by intestinal endopeptidases in the gastrointestinal tract. The resulting gliadin peptides cross the intestinal epithelium into the *lamina propria via* transcellular and paracellular pathways.[4] Within the extracellular matrix of the *lamina propria*, gliadin peptides such as the specific 33-mer α-gliadin peptide (P56–88) are modified by the calcium-dependent enzyme transglutaminase 2 (TG2) through deamidation and transamidation (crosslinking). This mechanism significantly enhances the immunogenicity of P56–88 by increasing its affinity for the HLA-DQ2 receptor on antigen-presenting cells.[5–7] In addition, TG2 is expressed by intestinal epithelial cells and is considered to facilitate the uptake of gliadin peptides.[8–12] The final immune cascade is characterized by the production of CD-specific anti-TG2-IgA-autoantibodies and the release of the Th1-cytokines IFN-γ and TNF-α. Ultimately, this process results in the destruction of the intestinal mucosa leading to malabsorption and diverse extraintestinal symptoms. In contrast, the peptide P31–49 mediates direct inflammatory effects mainly *via* the innate immune system.[13]

Currently, the only effective treatment for CD is a strict lifelong gluten-free diet, which involves the rigorous elimination

[a]*Department of General Pediatrics and Neonatology, Justus Liebig University Giessen, Feulgenstrasse 12, Giessen, Germany.*
E-mail: andrea.diers-1@ernaehrung.uni-giessen.de; Tel: +49 641 985 46601
[b]*Department of Nutritional Science, Justus Liebig University Giessen, Wilhelmstrasse 20, Giessen, Germany*
[c]*Center for Sustainable Food Systems, Justus-Liebig-University Giessen, Senckenbergstrasse 3, Giessen, Germany*
[d]*Department of Organic Chemistry, Justus Liebig University Giessen, Heinrich-Buff-Ring 17, Giessen, Germany*

of gluten-containing food. While this approach can alleviate symptoms and promote intestinal healing, it represents a significant challenge for patients and their families due to the dietary restrictions and the related social and economic burden.[14,15] This contributes to a significantly impaired quality of life in CD patients and reduced rates of dietary adherence (about 75% of patients), especially in adolescents and patients with subtle symptoms.[16,17] These facts underscore the high need for supplementary therapeutic options apart from the gluten-free diet.

Recent research has indicated that anthocyanins (ACN), certain naturally occurring secondary plant compounds might have a positive influence in the context of CD due to their anti-inflammatory and antioxidant properties and their ability to bind gliadin peptides.[18–23] ACN are water-soluble vacuolar pigments found in fruits and vegetables, giving them their characteristic red to blue color. In edible plants, cyanidin-3-glucoside (C3G) and delphinidin-3-glucoside (D3G) are the most common ACN.[24] There is some evidence from cell culture-based studies that ACN mitigate CD-associated inflammation.[25–27] However, functional studies exploring the possible molecular background in an inflammatory setting are scarce. In this study, we aimed to investigate effects of the ACN C3G and D3G on TG2-mediated crosslinking of gliadin and on IFN-γ- and TNF-α-mediated inflammatory effects in human intestinal cells.

Materials and methods

Anthocyanin preparation

The anthocyanins (ACN) cyanidin-3-glucoside (C3G; 1201-3) and delphinidin-3-glucoside (D3G; 1401-3) were obtained from Polyphenols AS (Sandnes, Norway). The lyophilized extract was prepared as a stock solution in Tris-buffer containing 50 mmol L^{-1} Tris, 1 mmol L^{-1} EDTA, 5 mmol L^{-1} calcium chloride, and 10 mmol L^{-1} dithiothreitol (DTT) (pH 7.5) or in cell culture medium immediately before use. To ensure complete dissolution, the stock solution was subjected to ultrasonic treatment in an ice-cooled bath for 3 minutes. The stock solution was subsequently diluted to the working concentrations for experimental use. The ACN concentrations of 50 μmol L^{-1} and 100 μmol L^{-1} were selected to reflect physiological achievable intestinal luminal exposure following consumption of ACN-rich food.

TG2-mediated crosslinking of gliadin peptides

For *in vitro* crosslinking experiments, a 96-well microplate was coated with 10 nmol L^{-1} transglutaminase 2 (TG2; T022, Zedira, Darmstadt, Germany) in Tris-buffer with 10 mmol L^{-1} DTT (99%, Sigma-Aldrich, Darmstadt, Germany) for 1 hour at 37 °C. Then, the wells were washed three times with PBS and subsequently blocked with 2% bovine serum albumin (BSA) in PBS for 30 minutes at room temperature. After blocking, the wells were incubated for 1 hour at 37 °C with 10 μg mL^{-1} commercially available pepsin-trypsin-digested gliadin (PTG; P004, Zedira) or biotinylated gliadin peptide P56–88 (G009, Biosynth, Staad, Switzerland; chemical structure: H-LQLQPFPQPQLPYPQPQLPYPQPQLPYPQPQPF-OH) in the presence or absence of 50 and 100 μmol L^{-1} of the ACN C3G or D3G. The irreversible TG2-specific inhibitor ERW1041 (Merck KGaA, Darmstadt, Germany) served as a control. After three washing steps, a primary antibody specific for gliadin (clone XGY4, Zedira) diluted 1 : 1000 in 2% BSA was applied to samples containing PTG and incubated overnight at 4 °C on an orbital shaker. Thereafter, a secondary, horseradish peroxidase-conjugated antibody targeting mouse IgG (sc-516102, Santa Cruz Biotechnology, Dallas, Texas, USA) diluted 1 : 1000 in 2% BSA was added to the wells and incubated for 1 hour at room temperature on an orbital shaker. When biotinylated P56–88 was used, the wells were incubated with horseradish peroxidase-conjugated streptavidin (streptavidin-HRP; BioLegend, San Diego California, USA) diluted 1 : 2500 in 2% BSA on an orbital shaker at 4 °C overnight. After three washes with PBS, tetramethylbenzidine substrate (TMB; Sigma-Aldrich) was added to each well. Following a 15-minute incubation, photometric quantitation was performed at 655 nm using a Clariostar Plus (BMG Labtech) microplate reader. As a comparative test, the experiment was also conducted with 5BP (Thermo Fisher Scientific, Langenselbold, Germany) and 100 μmol L^{-1} ACN. Again, streptavidin-HRP and TMB substrate were used for photometric evaluation.

To investigate the effects of ACN on TG2 activity at different calcium concentrations, Tris-buffers with different concentrations ranging from 0 to 5 mmol L^{-1} were used. In this assay, TG2-mediated crosslinking of the transglutaminase substrate 5-biotinamidopentylamine (5BP; 500 μmol L^{-1}, 21345, Thermo Fisher Scientific) was detected by streptavidin-HRP as described above.

Cell culture

Human intestinal epithelial cells (Caco-2; ATCC HTB-37, Manassas, Virginia, USA) were cultured at 37 °C with 5% CO_2 and 95% humidity in Dulbeccos Modified Eagle Medium (DMEM; Thermo Fisher Scientific) supplemented with 1% penicillin–streptomycin, 1% non-essential amino acids, 1% sodium pyruvate (all Thermo Fisher Scientific), and 10% heat-inactivated fetal bovine serum (FBS; Thermo Fisher Scientific, LOT B2724126RP). The culture medium was replaced every two to three days and cells were passaged at 60 to 80% confluence using TrypLE express (Thermo Fisher Scientific).

Extracellular TG2 activity in Caco-2 cells

To investigate the effect of ACN on the extracellular TG2 activity, 2×10^4 Caco-2 cells were seeded on a 96-well microplate and used 4 to 7 days after confluency, to ensure sufficient differentiation of the cell monolayer as well as reliable viability and activity measurement without late differentiation and contact inhibition possibly changing the metabolic profile. The non-permeabilized cells were incubated with 5BP in Tris-buffer in the presence of ACN (50 and 100 μmol L^{-1}) or ERW1041 (100 μmol L^{-1}).

After incubation, the cells were washed with PBS, fixed with 4% paraformaldehyde for 10 min and blocked with 5% BSA in PBS at 4 °C overnight. The next day, cells were incubated at room temperature with streptavidin-Alexa488 (2 μg mL^{-1}, Thermo Fisher Scientific) in 5% BSA for 1 hour in the dark and subsequently washed with PBS three times. Fluorometric quantitation was conducted using Clariostar Plus microplate reader (BMG Labtech, excitation 488 nm, emission 535 nm). The data were background subtracted against a control without 5BP substrate.

Nuclear magnetic resonance (NMR) spectroscopy

To investigate possible interactions between TG2 and the ACN, Saturation Transfer-Difference (STD) ^{1}H-NMR experiments were performed with solvent suppression. The TG2–ACN mixtures were prepared in D_2O (99.9%, Carl Roth, Karlsruhe, Germany) in a 1 : 100 molar ratio.[28] The mixtures contained 80 μg mL^{-1} TG2 (corresponding to approximately 1 μmol L^{-1}) and 100 μmol L^{-1} of C3G or D3G. Before transferring the samples into NMR tubes, they were filtered through a 0.2 μm filter (Cytivia, Marlborough, USA).

The NMR measurements were recorded on a Bruker 700 MHz Avance Neo spectrometer equipped with a 5 mm TCI *z*-gradient prodidy probe. The chemical shifts were measured in ppm. All NMR measurements were performed at 298 K. The data were processed and analyzed using TopSpin 4.1 from Bruker BioSpin.

Cell viability of Caco-2

The viability of Caco-2 cells was assessed using the PrestoBlue HS assay (Thermo Fisher Scientific). 2×10^4 Caco-2 cells per well were seeded on a 96-well microplate. Again, the cells were used 4 to 7 days after confluency to ensure complete differentiation with reliable activity measurement. The cells were treated with interferon-γ (IFN-γ; 1000 IU mL^{-1}, Sigma-Aldrich, Darmstadt, Germany) or tumor necrosis factor-α (TNF-α; 20 ng mL^{-1}, Thermo Fisher Scientific) with or without addition of C3G or D3G (1, 10, 50, 100 and 200 μmol L^{-1}). Incubation was performed for 24 hours in cell culture medium at 37 °C. Afterwards, cells were washed once with PBS and incubated with PrestoBlue HS reagent (diluted 1 : 10 in culture medium) for 2 hours at 37 °C. Fluorescence was measured using a Clariostar Plus (BMG Labtech, Ortenberg, Germany) microplate reader (excitation at 545 nm, emission at 600 nm).

Quantitative real-time PCR (qRT-PCR)

Caco-2 cells were seeded at a density of 1×10^5 cells per well on a 24-well microplate. The cells were used 10 to 12 days after reaching confluency which is enough time to ensure stable expression of enterocyte specific genes and proteins. Naïve Caco-2 cells and Caco-2 cells stimulated with IFN-γ (1000 IU mL^{-1}) or TNF-α (20 ng mL^{-1}) were incubated with C3G and D3G (100 μmol L^{-1}) in culture medium for 24 hours at 37 °C. Following treatment, the cell culture medium was removed, the cells were washed twice with ice-cold PBS, detached using TrypLE express and centrifuged at 14 100*g* for 60 seconds. The cell pellets were frozen at −80 °C for subsequent RNA extraction.

Total RNA was extracted from the pellets using the RNeasy Mini Kit (Qiagen, Hilden, Germany) according to the manufacturer's instructions. The RNA concentration was measured using a Clariostar Plus microplate reader. To analyze mRNA levels of TG2, the extracted RNA was reverse transcribed into complementary DNA using the QuantiTect Reverse Transcription Kit (Qiagen) in accordance with the manufacturer's protocol. Quantitative Real-Time PCR (qPCR) was performed using the 7500 Real-Time PCR System (Thermo Fisher Scientific) with SYBR Green Master Mix (Quantabio, Beverly, Massachusetts, USA) according to a standard protocol. The temperature and time conditions used are shown in Table 1.

The following primers were used for TG2: forward primer sequence: 5′-TGTGGCACCAAGTACCTGCTCA-3′ and reverse primer sequence: 5′-GCACCTTGATGAGGTTGGACTC-3′ (Thermo Fisher Scientific). GAPDH was used as a housekeeping gene (forward primer sequence: 5′-GTCTCCTCTGACTTCAACAGEG-3′; reverse primer sequence: 5′-ACCACCCTGTTGCTGTAGCCAA-3′, Thermo Fisher Scientific). Each PCR reaction (20 μL) consisted of 10 μL SYBR Green Master Mix, 1 μL cDNA, 1 μL of each primer and nuclease-free water. All samples were run in triplicates and to confirm specificity, a melting curve analysis was conducted. The housekeeping gene GAPDH was used as an internal control to normalize RNA input. Relative gene expression was calculated using the $2^{-\Delta\Delta CT}$ method (ΔCt = Ct (target) − Ct (housekeeping)).

Western blotting

Caco-2 cells were seeded at a density of 1×10^5 cells per well on a 24-well microplate. The cells were used 10 to 12 days after reaching confluency. Naïve cells as well as cells stimulated with IFN-γ (1000 IU mL^{-1}) or TNF-α (20 ng mL^{-1}) were incubated with C3G or D3G (100 μmol L^{-1}) in cell culture medium for 48 hours at 37 °C. Following treatment, the cells were harvested as described for qRT-PCR. The resulting cell pellets were washed twice with PBS and resuspended in radioimmunoprecipitation lysis buffer (RIPA, sc-24948, Santa Cruz Biotechnology, USA) supplemented with phenylmethylsulfonyl fluoride (PMSF), protease inhibitors, and sodium orthovanadate (1% each). The lysis was carried out on ice for 20 minutes, followed by centrifugation at 19 060*g* for 20 minutes at 4 °C. The supernatant was collected in a fresh tube and protein concentration was determined using the

Table 1 Real-time PCR thermal cycling conditions

Phase	Temperature (°C)	Time	Cycles
Initial denaturation	95	5 min	1
Denaturation	95	45 s	45
Annealing	58	30 s	45
Elongation	72	30 s	45
Melt curve	95; 60 (multilevel)	15–20 s each	1

Pierce BCA Protein Assay Kit (23225, Thermo Fisher Scientific) according to the manufacturer's instructions.

For western blot analysis, Laemmli buffer containing 2-mercaptoethanol was added to the samples, which were then denatured at 95 °C for 5 minutes. Proteins (10 μg per lane) were separated using 10% SDS-PAGE at 40 mA. Subsequently, the proteins were transferred onto a nitrocellulose membrane with a 0.2 μm pore size using the trans-Blot Turbo system (Bio-Rad Laboratories, Feldkirchen, Germany) for 30 minutes. After blocking, the membrane was incubated overnight at 4 °C with a primary antibody against transglutaminase 2 (TGM2 mAb, clone D11A6, Cell Signaling Technology, Danvers, USA) diluted 1 : 2000. A secondary anti-rabbit antibody (m-rabbit, 01/2029, Cell Signaling Technology) was used with a dilution of 1 : 1000. For detection of GAPDH as a non-regulated protein for normalization, the blots were first stripped (Restore™ Western Blot Stripping Buffer, 21063, Thermo Fisher Scientific) and then incubated with a primary antibody against glyceraldehyde-3-phosphate dehydrogenase (MAB374, Merck KGaA) diluted 1 : 5000 and m-IgGκ BP-HRP as secondary antibody (sc-516102, Santa Cruz Biotechnology) diluted 1 : 1000.

In silico molecular affinity experiments

Molecular docking experiments were performed using the web-based tool CB-Dock2 (https://cadd.labshare.cn/cb-dock2/php/blinddock.php, assessed 23/05/2025), which employs cavity detection-guided blind docking to predict ligand–protein interactions.[29] The molecular structures of TG2 in an active, open conformation (2Q3Z), the IFN-γ/IFN-γR1/IFN-γR2-hexamer (6E3L) and the TNF-α/TNF-α-R2-complex (3ALQ) were obtained from the Protein Data Base and 3D conformers of the ligands C3G and D3G were obtained from the PubChem database. CB-Dock2 automatically detected potential binding cavities within the receptors and generated docking poses using Auto BlindDock as the scoring engine. For each cavity, multiple docking conformations were calculated, and the top-ranked poses were selected based on Vina docking scores and predicted binding orientation. Higher negative Vina scores indicated stronger binding of the ligand with values more than −4 kcal mol^{-1} and more than −8 kcal mol^{-1} indicating moderate and strong affinity respectively. Docking results were visualized and analyzed to evaluate binding modes and potential molecular interactions.

Statistics

Statistical analysis was performed using Graph-Pad Prism 10 (GraphPad Prism Software Inc., La Jolla, CA, USA). All data was tested for normality of distribution of the residuals applying Shapiro–Wilk test and for heteroscedasticity applying Spearman's rank correlation test (predicted Y *vs.* |residual|). In case of normally distributed residuals with variance homogeneity, a two-way RM ANOVA followed by Dunnett's or Šidák's test was performed, as both the dependencies within the biological replicates and the treatments themselves represent influencing factors and because the cells of a biological repetition originate from the same stock and passage. For non-normally distributed residuals, a sensitivity analysis was performed to verify the robustness of the results by comparing the significance values with and without outliers. In case of heteroscedasticity, the data was transformed accordingly. Statistical significance was accepted at $p < 0.05$.

Results

Anthocyanins can inhibit the activity of recombinant TG2

As enzymatic modification of gliadin peptides by TG2 plays such an essential role in the pathogenesis of CD, we first investigated whether ACN interfere with this process. For this purpose, we analyzed the effect of different concentrations of C3G or D3G on TG2-mediated crosslinking of a pepsin–trypsin–digested gliadin (PTG) on an *in vitro* level. D3G significantly reduced the crosslinking by recombinant TG2 when used at a concentration of 100 μmol L^{-1} (to 46 ± 18%, $p < 0.05$, Fig. 1A). C3G did not show a significant effect (100 μmol L^{-1}: 60 ± 23%, $p = 0.23$). To further evaluate this observation, we compared the influence of both ACN with the effect of the active site-directed, irreversible TG2-inhibitor ERW1041. This specific inhibitor reduced TG2-activity to 13 ± 7% ($p < 0.001$).

We also performed a similar experiment using the specific potentially immunogenic gliadin peptide P56–88. This peptide is the key target of TG2-mediated deamidation and is known to induce the Th1-dominated immune response observed in CD. Here, neither of the two ACN had a significant effect (C3G 100 μmol L^{-1}: 51 ± 19%, $p = 0.13$; D3G 100 μmol L^{-1}: 71 ± 12%, $p = 0.16$), whereas ERW1041 significantly reduced TG2-activity to 25 ± 22% ($p < 0.05$) (Fig. 1B).

We further performed an experiment using the substance 5BP instead of gliadin as a TG2 substrate. Here, C3G decreased 5BP crosslinking to 47 ± 30% ($p < 0.05$) whereas D3G had no significant effect (57 ± 26%, $p = 0.1$). This finding argued against the observed effect being rooted in a specific molecular interaction between the ACN and gliadin. Treatment with ERW1041 led to a decline to 26 ± 14% ($p < 0.01$) (Fig. 1C).

We next applied a cell-culture model based on the intestinal epithelial cell line Caco-2 to further investigate the effect of ACN on the extracellular TG2 activity. In detail, we analyzed the influence of C3G and D3G on TG2-mediated crosslinking of the substrate 5BP in unpermeabilized Caco-2 cells. After a 3-hour incubation, ERW1041 significantly reduced the TG2 activity to 63 ± 6% ($p < 0.01$) (Fig. 2A). After 30 minutes of incubation, ERW1041 significantly reduced the TG2 activity to 75 ± 11% ($p < 0.05$), whereas neither of the ACN showed an effect (D3G 100 μmol L^{-1}: 86 ± 7%, $p = 0.33$) (Fig. 2B).

C3G and D3G bind directly to TG2, primarily *via* their glucoside residue

Next, we aimed to further investigate the mechanism by which C3G and D3G interfere with TG2 enzymatic activity. We hypothesized that a direct molecular interaction of ACN with TG2 might affect its enzymatic function. First, we performed

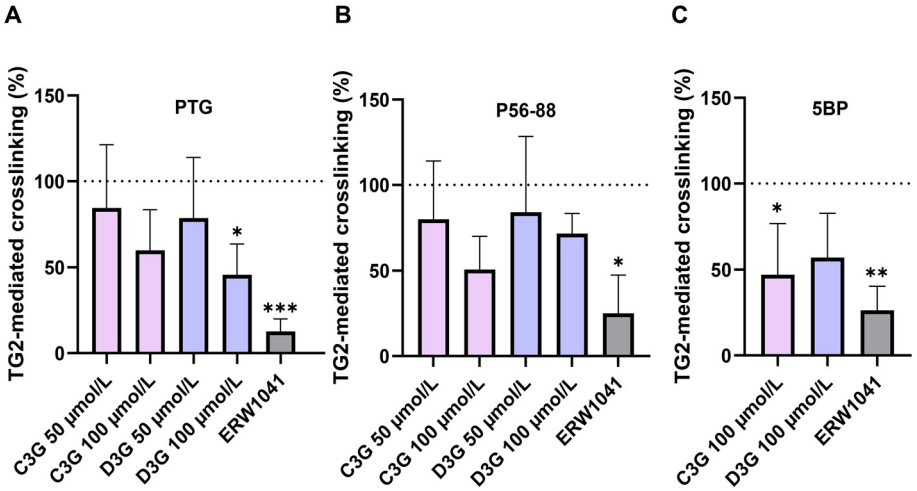

Fig. 1 Crosslinking of PTG, P56–88 and 5BP by recombinant TG2. TG2-mediated crosslinking of (A) pepsin–trypsin–digested gliadin (PTG; n = 5), (B) gliadin peptide P56–88 (n = 4) and (C) the TG2 substrate 5-biotinamidopentylamine (5BP; n = 5) was quantified photometrically. Two technical replicates per condition were done. Data is shown as mean ± standard deviation. Normalized data is shown, the dashed line indicates the TG2 control (100%). Statistical significance was tested using two-way RM ANOVA followed by Dunnett's test using the non-normalized raw data. * indicates significant difference to untreated control; * $p < 0.05$; ** $p < 0.01$; *** $p < 0.001$.

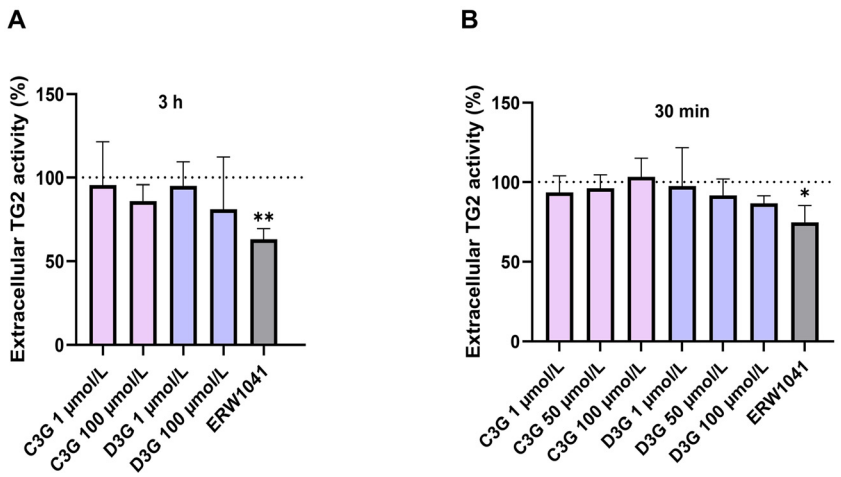

Fig. 2 Effect of ACN on extracellular TG2 activity of Caco-2 cells. Extracellular TG2 activity on Caco-2 monolayers was tested using 5BP as a substrate. Data is shown as mean ± standard deviation of 4 independent experiments. Normalized data is shown, the dashed line indicates the 5BP treated control (100%). Statistical significance was tested using two-way RM ANOVA followed by Dunnett's test using the non-normalized raw data. The residues of the 30-minute data were not normally distributed, so a sensitivity analysis was performed excluding an outlier from the D3G 100 µmol L^{-1} treatment. The sensitivity analysis confirmed the robustness of the results. * $p < 0.05$; ** $p < 0.01$.

NMR experiments in order to investigate whether there is a spatial relationship between ACN and TG2.

STD-NMR is suited to receptor proteins with large masses. Macromolecules with large molecular masses possess large rotational correlation times τ_c that enhance spin diffusion and, consequently, protons that are in close contact with the receptor (≤5 Å) and therefore involved in the binding process to receive magnetization transfer leading to STD-NMR signals. Molecules that bind to the protein (*e.g.* C3G and D3G) then get saturated through the binding location. In the difference STD spectrum, only the signals of the molecules that bind to the protein are present.[21,30] The ^{1}H spectrum of C3G and D3G (Fig. 3A and B), revealed small peaks in the range of 6 to 9 ppm (aromatic protons of the ACN). In the case of D3G, these were only slightly visible (see zoomed-in view). Strong signals were detected at 3 to 4 ppm deriving from the glucoside part of the ACN. In comparison, the ^{1}H spectrum of the mixture of TG2 and ACN showed an additional peak between 5 and 5.5 ppm, while less signal appeared in the range from 1 to 1.5 and 6 to 9 ppm. We used STD NMR-spectroscopy for a detailed investigation of the residues of C3G and D3G that are involved in the interaction with TG2. This analysis revealed

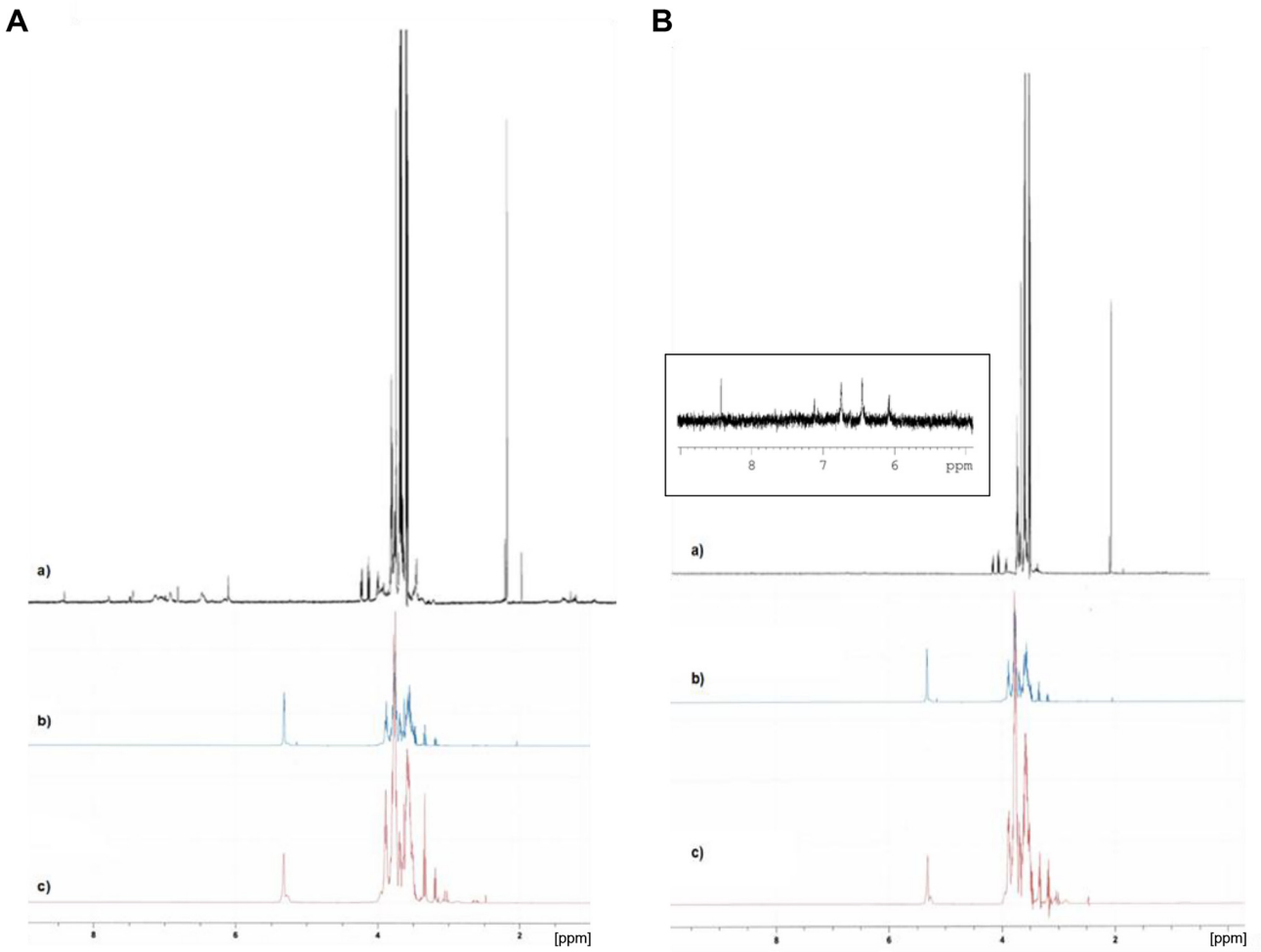

Fig. 3 (A) NMR spectra of TG2 with C3G at pH 7.4. (a) ^{1}H NMR spectrum of C3G in D_2O, (b) ^{1}H NMR spectrum of C3G and TG2 in D_2O, (c) STD spectrum of C3G and TG2 in D_2O. (B) NMR spectra of TG2 with D3G at pH 7.4 (a) ^{1}H NMR spectrum of D3G in D_2O, (b) ^{1}H NMR spectrum of D3G and TG2 in D_2O, (c) STD spectrum of D3G and TG2 in D_2O.

distinct peaks between 3 to 4 ppm representing the glucoside ring and between 5 to 5.5 ppm representing the anomeric proton, which is bound to the C-1 carbon of the sugar ring (Fig. 3A and B, panel c). These findings indicated a molecular interaction of C3G and D3G with TG2 which is mediated by the glucoside moiety of the ACN.

C3G and D3G interfere with calcium-mediated activation of TG2

Next, we performed molecular docking experiments to address the question at which sites ACN interact with TG2. In total, five binding sites between C3G or D3G and TG2 were identified with relevant Vina scores indicating a moderate to high affinity (Fig. 4A and B). Binding sites and the corresponding contact residues of TG2 were comparable between C3G and D3G. For both ACN, docking analysis revealed a similar binding site with high affinity (<−8 kcal mol^{-1}, C2) and several other binding sites with moderate affinities (−4 to −8 kcal mol^{-1}). None of the identified binding sites revealed a relationship to the active center (cysteine 277, histidine 335, aspartic acid 358). However, the identified binding sites with the highest affinities (C2 and C4) revealed a spatial relationship with calcium-binding sites which have been previously published.[31–33] Thereafter, we investigated the effect of C3G and D3G on calcium-mediated activation of recombinant TG2. For this purpose, we analyzed crosslinking of the transglutaminase-substrate 5BP by TG2. At low calcium-concentrations below 2 mmol L^{-1}, there was no measurable enzymatic activity of TG2. However, at a concentration of 2 mmol L^{-1} calcium and higher, TG2 activity was significantly increased and reached a plateau at a concentration of 3 mmol L^{-1}. Regarding the effects of ACN on calcium-mediated activation of TG2, there was no significant effect of C3G at the tested concentrations of 100 μmol L^{-1}. However, D3G reduced TG2-activity to 51 ± 23% (4 mmol L^{-1} calcium, $p < 0.01$) and 58 ± 27% (5 mmol L^{-1} calcium, $p < 0.05$) and thus showed an increased efficiency at higher calcium concentrations (Fig. 4C).

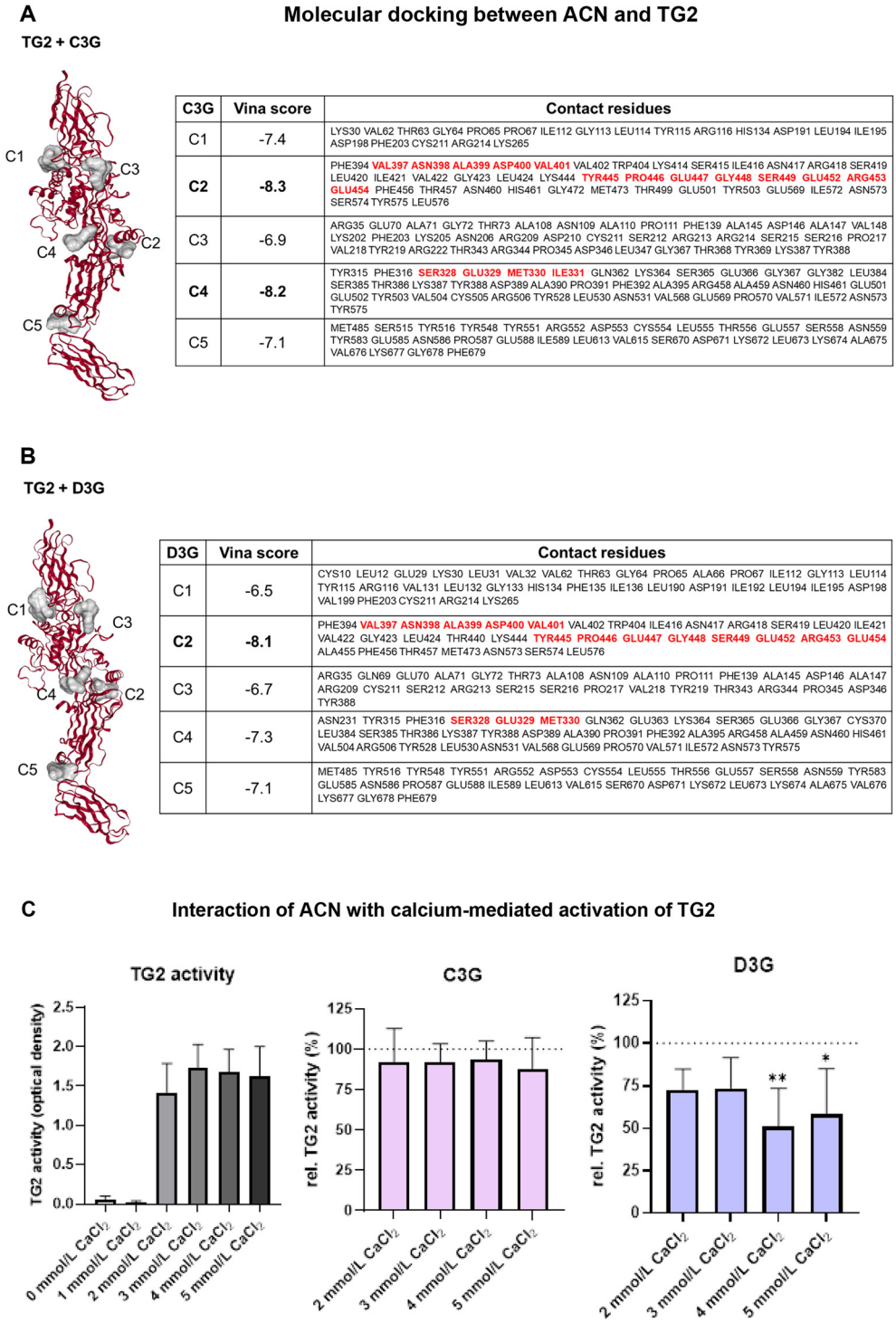

C3G	Vina score	Contact residues
C1	-7.4	LYS30 VAL62 THR63 GLY64 PRO65 PRO67 ILE112 GLY113 LEU114 TYR115 ARG116 HIS134 ASP191 LEU194 ILE195 ASP198 PHE203 CYS211 ARG214 LYS265
C2	**-8.3**	PHE394 **VAL397 ASN398 ALA399 ASP400 VAL401** VAL402 TRP404 LYS414 SER415 ILE416 ASN417 ARG418 SER419 LEU420 ILE421 VAL422 GLY423 LEU424 LYS444 **TYR445 PRO446 GLU447 GLY448 SER449 GLU452 ARG453 GLU454** PHE456 THR457 ASN460 HIS461 GLY472 MET473 THR499 GLU501 TYR503 GLU569 ILE572 ASN573 SER574 TYR575 LEU576
C3	-6.9	ARG35 GLU70 ALA71 GLY72 THR73 ALA108 ASN109 ALA110 PRO111 PHE139 ALA145 ASP146 ALA147 VAL148 LYS202 PHE203 LYS205 ASN206 ARG209 ASP210 CYS211 SER212 ARG213 ARG214 SER215 SER216 PRO217 VAL218 TYR219 ARG222 THR343 ARG344 PRO345 ASP346 LEU347 GLY367 THR368 TYR369 LYS387 TYR388
C4	**-8.2**	TYR315 PHE316 **SER328 GLU329 MET330 ILE331** GLN362 LYS364 SER365 GLU366 GLY367 GLY382 LEU384 SER385 THR386 LYS387 TYR388 ASP389 ALA390 PRO391 PHE392 ALA395 ARG458 ALA459 ASN460 HIS461 GLU501 GLU502 TYR503 VAL504 CYS505 ARG506 TYR528 LEU530 ASN531 VAL568 GLU569 PRO570 VAL571 ILE572 ASN573 TYR575
C5	-7.1	MET485 SER515 TYR516 TYR548 TYR551 ARG552 ASP553 CYS554 LEU555 THR556 GLU557 SER558 ASN559 TYR583 GLU585 ASN586 PRO587 GLU588 ILE589 LEU613 VAL615 SER670 ASP671 LYS672 LEU673 LYS674 ALA675 VAL676 LYS677 GLY678 PHE679

D3G	Vina score	Contact residues
C1	-6.5	CYS10 LEU12 GLU29 LYS30 LEU31 VAL32 VAL62 THR63 GLY64 PRO65 ALA66 PRO67 ILE112 GLY113 LEU114 TYR115 ARG116 VAL131 LEU132 GLY133 HIS134 PHE135 ILE136 LEU190 ASP191 ILE192 LEU194 ILE195 ASP198 VAL199 PHE203 CYS211 ARG214 LYS265
C2	**-8.1**	PHE394 **VAL397 ASN398 ALA399 ASP400 VAL401** VAL402 TRP404 ILE416 ASN417 ARG418 SER419 LEU420 ILE421 VAL422 GLY423 LEU424 THR440 LYS444 **TYR445 PRO446 GLU447 GLY448 SER449 GLU452 ARG453 GLU454** ALA455 PHE456 THR457 MET473 ASN573 SER574 LEU576
C3	-6.7	ARG35 GLN69 GLU70 ALA71 GLY72 THR73 ALA108 ASN109 ALA110 PRO111 PHE139 ALA145 ASP146 ALA147 ARG209 CYS211 SER212 ARG213 SER215 SER216 PRO217 VAL218 TYR219 THR343 ARG344 PRO345 ASP346 TYR388
C4	-7.3	ASN231 TYR315 PHE316 **SER328 GLU329 MET330** GLN362 GLU363 LYS364 SER365 GLU366 GLY367 CYS370 LEU384 SER385 THR386 LYS387 TYR388 ASP389 ALA390 PRO391 PHE392 ALA395 ARG458 ALA459 ASN460 HIS461 VAL504 ARG506 TYR528 LEU530 ASN531 VAL568 GLU569 PRO570 VAL571 ILE572 ASN573 TYR575
C5	-7.1	MET485 TYR516 TYR548 TYR551 ARG552 ASP553 CYS554 LEU555 THR556 GLU557 SER558 ASN559 TYR583 GLU585 ASN586 PRO587 GLU588 ILE589 LEU613 VAL615 SER670 ASP671 LYS672 LEU673 LYS674 ALA675 VAL676 LYS677 GLY678 PHE679

Fig. 4 Molecular docking of (A) C3G or (B) D3G and TG2. A 3D-reconstruction of the 5 binding sites and the corresponding Vina scores for binding affinity and contact residues are shown. Contact residues with functional significance are highlighted in red. (C) Calcium-mediated activation of recombinant TG2 and the effect of 100 μmol L^{-1} C3G and 100 μmol L^{-1} D3G (n = 4). Data is shown as mean ± standard deviation. Normalized data is shown, the dashed line indicates the control (100%). Statistical significance was tested using two-way RM ANOVA followed by Šidák's test using the non-normalized raw data. * $p < 0.05$; * $p < 0.01$.

C3G and D3G improve cell viability under IFN-γ and TNF-α exposure

Then, we investigated whether ACN mitigate inflammatory effects of CD-associated cytokines IFN-γ and TNF-α in our cell culture model. For this purpose, cell viability of Caco-2 cells was quantified using a resazurin-based assay after simultaneous incubation with cytokines and ACN. In unstimulated Caco-2 cells, neither C3G nor D3G showed an effect on cell viability. Treatment with IFN-γ or TNF-α did not significantly impair cell viability. C3G and D3G at the concentrations of 10, 50, 100 and 200 μmol L^{-1} may have beneficial effects on cell viability in IFN-γ-stimulated Caco-2 cells while C3G at 10, 50 and 100 μmol L^{-1} significantly increased cell viability in TNF-α-stimulated cells (Fig. 5A and B).

C3G and D3G reduce TG2-expression in IFN-γ-stimulated Caco-2 cells

We next addressed the question whether C3G and D3G might mitigate the inflammatory response associated with CD. For this purpose, we incubated Caco-2 cells with IFN-γ and TNF-α. Since upregulation of TG2-expression represents one of the cornerstones of CD inflammation, we investigated the TG2 mRNA level using qPCR. We did not observe an influence of C3G or D3G on TG2 expression under non-inflammatory conditions. After 24 hours of stimulation with IFN-γ, however, TG2 mRNA levels were significantly increased by more than 3-fold. Simultaneous incubation with D3G attenuated this effect and reduced IFN-γ-mediated stimulation of TG2

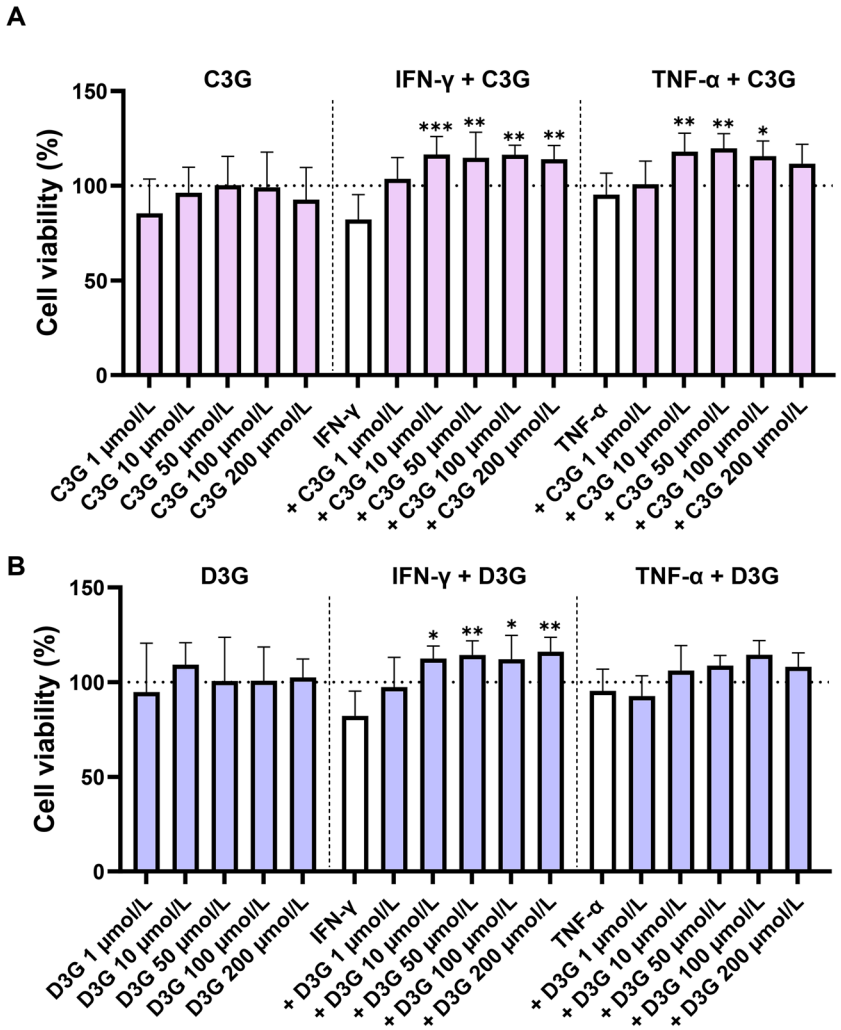

Fig. 5 Effects of ACN and cytokines on the viability of Caco-2 cells. The cell viability of Caco-2 cells was tested after 24-hour treatment with (A) C3G and (B) D3G alone and with addition of IFN-γ and TNF-α at the indicated concentrations. Five independent experiments were done with two technical replicates per condition. Data normalization was conducted relative to untreated controls (no cytokine or ACN treatment). Data is shown as mean ± standard deviation. Normalized data is shown, the dashed line indicates the untreated control (100%). Statistical significance was tested using two-way RM ANOVA followed by Šidák's test using the non-normalized raw data. The residues of the D3G data were not normally distributed, so a sensitivity analysis was performed excluding an outlier from the control group, which confirmed the robustness of the results. * $p < 0.05$; ** $p < 0.01$; *** $p < 0.001$ (cytokine *vs.* cytokine with ACN).

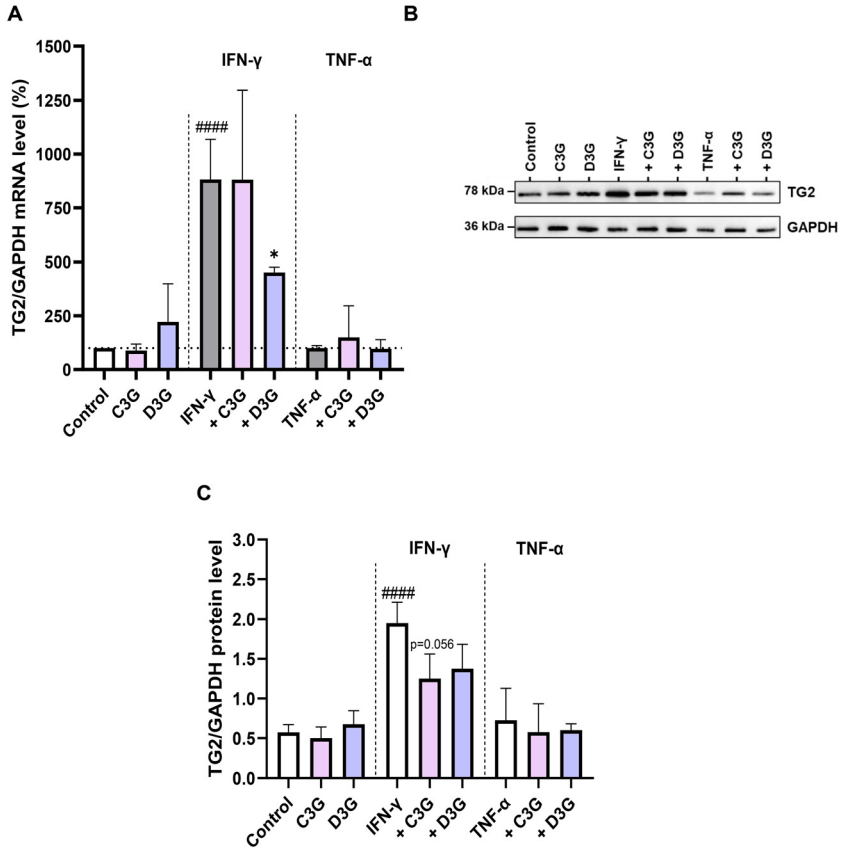

Fig. 6 Effects of ACN on cytokine-induced expression of TG2. Caco-2 cells were stimulated with IFN-γ or TNF-α and incubated with or without ACN (100 μmol L^{-1}). (A) The TG2 mRNA expression was determined by real-time PCR. GAPDH served as a housekeeping gene. Three independent experiments were done. (B) The TG2 protein level in whole cell lysates was determined by western blotting. Here, a representative western blot is shown, GAPDH served as a loading control for normalization. (C) The densitometric evaluation of western blots is given. Four independent experiments were done. Data is shown as mean ± standard deviation. To account for heteroscedasticity, mRNA level data was square-root transformed and protein level data was transformed using the natural logarithm. Statistical significance was tested using two-way RM ANOVA followed by Šidák's test using normalized data (mRNA level) or non-normalized raw data (protein level), respectively. $^{\#\#\#\#}$ $p < 0.0001$ (untreated controls *vs.* IFN-γ-stimulation); * $p < 0.05$ (IFN-γ-stimulation *vs.* IFN-γ with ACN).

expression to 51 ± 25% ($p < 0.05$). In contrast, C3G did not have any influence (Fig. 6A).

We next performed western blotting to analyze the TG2 protein levels 48 hours after cytokine stimulation. Treatment with C3G or D3G did not affect the expression of TG2. Incubation with 1000 IU mL^{-1} IFN-γ revealed a fourfold increase in TG2 protein levels (Fig. 6B and C). Although co-incubation with C3G or D3G did not significantly diminish the stimulatory effect of IFN-γ, the reduction observed with C3G (65 ± 20%, $p = 0.056$) is of interest. Given the borderline *p*-value and limited sample size, this finding may require cautious interpretation. D3G lead to a reduction to 71 ± 18% ($p = 0.17$). Incubation with 20 ng mL^{-1} TNF-α did not influence the expression of TG2 (Fig. 6B and C).

We hypothesized that a molecular interaction between ACN and the cytokines might interfere with their receptor binding, which might be the cause of the mitigation of their inflammatory effects. We thus performed *in silico* analyses to investigate the molecular interactions between C3G or D3G, IFN-γ or TNF-α and their corresponding receptors. The IFN-γ receptor complex is a hexameric complex that is composed of IFN-γ, and the transmembrane receptors IFN-γR1 and IFN-γR2 (2 : 2 : 2). The TNF-α receptor complex is a hexameric complex that contains the TNF-α homotrimer and three monomers of TNF-αR2. Protein–ligand blind docking was done using CB-Dock2.

In total, five similar binding sites for C3G and D3G and the IFN-γ receptor complex were identified. All binding sites were characterized by moderate to high Vina scores indicating a significant affinity between ACN and the cytokine receptor complex (Fig. 7). Among the potential interaction sites with high affinities, C1, C2 and C4 revealed multiple contact residues that are involved in the assembly of the IFN-γ receptor complex.[34,35]

Docking experiments with the TNF-α receptor complex and C3G or D3G revealed five similar binding sites with moderate to high affinity between the complex and the ACN. Among those, C1–C4 revealed multiple contact residues that are involved in the aggregation of the TNF-α receptor complex. Again, the binding sites and affinities of C3G and D3G were similar.

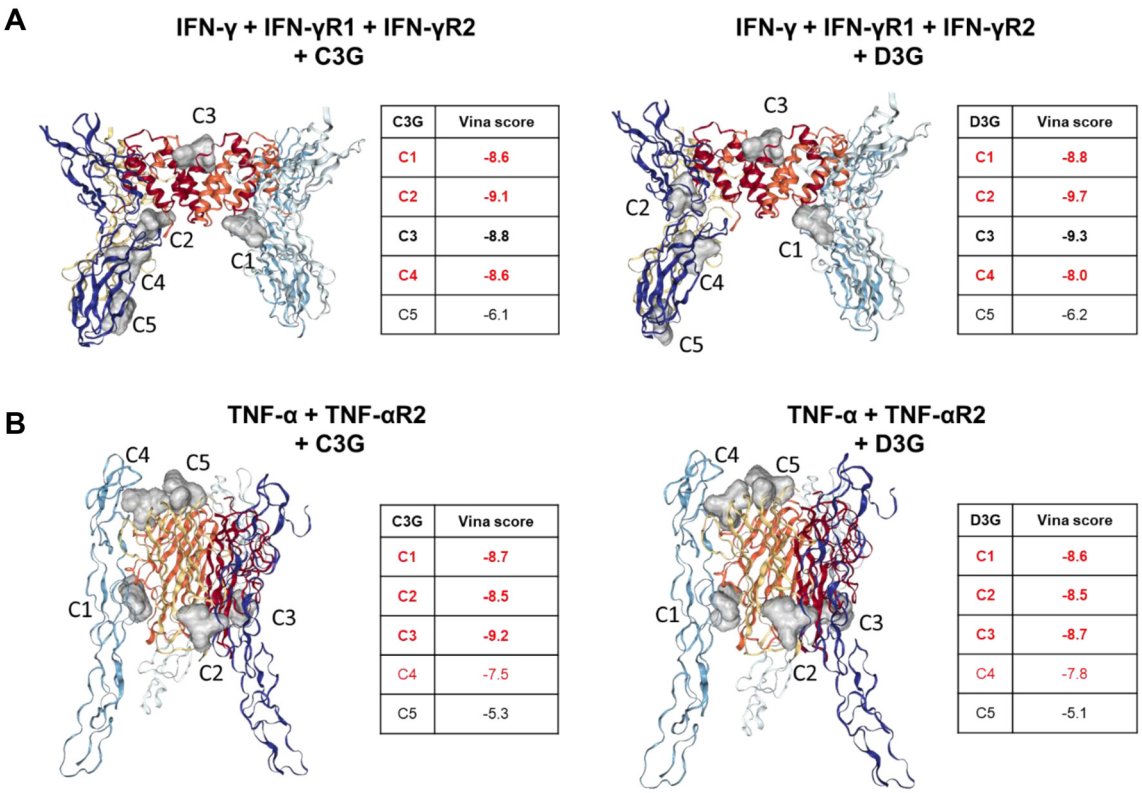

Fig. 7 Molecular docking of (A) the IFN-γ receptor complex (IFN-γ–IFN-γR1–IFN-γR2 hexamer) or (B) the TNF-α receptor complex (TNF-α + TNF-αR2 complex) and C3G or D3G. Shown is a 3D-reconstruction of the 5 binding sites of the IFN-γ receptor complex and C3G or D3G, respectively (red = IFN-γ chain A, orange = IFN-γ chain B, yellow = IFN-γR1 chain C, grey = IFN-γR1 chain D, light blue = IFN-γR2 chain E, dark blue = IFN-γR2 chain I) and a 3D-reconstruction of the 5 binding sites of the TNF-α receptor complex and C3G or D3G, respectively (red = TNF-α chain A, orange = TNF-α chain B, yellow = TNF-α chain C, grey = TNF-αR2 chain R, light blue = TNF-αR2 chain S, dark blue = TNF-αR2 chain T). Docking sites with high affinity (Vina score < −8 kcal mol^{-1}) are shown in bold. Docking sites with potential functional significance are highlighted in red.

Discussion

TG2 is the key enzyme in the pathogenesis of CD as it is responsible for the enzymatic modification of ingested gliadin peptides. Inhibition of TG2 is currently considered one of the most promising new strategies for the treatment of CD. In the past, various types of reversible and irreversible TG2 inhibitors have been investigated.[10,36,37] In addition to these synthetic TG2 inhibitors, it seems of great interest to investigate natural food compounds such as ACN found in high amounts in a variety of red and blue berries[20] regarding their potential to modulate TG2 activity. This would be of advantage due to their potentially high tolerability and additional health-promoting effects. In this study, we aimed to investigate whether and how the two major ACN, C3G and D3G, could influence the cross-linking activity of TG2 and the cellular inflammatory response after stimulation with the CD-associated cytokines IFN-γ and TNF-α.

Our *in vitro* experiments demonstrated that D3G can effectively inhibit TG2-mediated crosslinking of a gliadin peptide mixture at a concentration of 100 μmol L^{-1} (Fig. 1A). This emphasizes its potential to modulate TG2 function under physiologically relevant conditions, *i.e.* in concentrations which can be found in ACN-rich juices and smoothies.[18] The ACN doses used in this study were selected in accordance with similar cell culture studies in which ACN concentrations ranging from 1 μmol L^{-1} to several mmol L^{-1} were applied.[26,38–42] Bilberries and blackberries contain about 90 mg cyanidin and delphinidin per 100 g edible portion.[43] With a consumption of 150 g of berries, this would result in 135 mg of ACN. Considering the molecular weight of ACN (here approximately 490 g mol^{-1}) to calculate the amount of ACN that reach the intestine after such consumption, a concentration of 300 μmol L^{-1} would be obtained. Assuming an average intestinal volume of 340 mL,[44] the luminal ACN concentrations would therefore reach approximately 900 μmol L^{-1} in this example. This is further supported by the fact that the majority of ACN are not absorbed but remain in the gastrointestinal tract.[45] Even assuming substantial dilution, degradation and uneven distribution, local luminal concentrations of 50 to 100 μmol L^{-1} are physiologically plausible.

However, the shown effect could not be confirmed in a cellular environment. In Caco-2 cells, ACN treatment did not lead to significantly reduced extracellular TG2 activity (Fig. 2). This could be due to the higher complexity of the cellular system, in which ACN undergo rapid metabolism, chemical instability

and pH- or oxidation-dependent degradation. In this experiment, an early differentiation approach was intentionally chosen to minimize metabolic changes due to prolonged culture and contact inhibition. Typically, Caco-2 cells require 14 to 21 days after confluence to achieve full differentiation and high TEER values (500–1100 Ω cm^2).[46] However, in independent experiments we conducted, a TEER value of 500 Ω cm^2 was already reached approximately 3 to 4 days after seeding. Similar values were obtained in existing publications, while other studies use lower TEER values for confluent monolayers.[47–53] Additionally, TG2 is constitutively expressed in Caco-2 cells under standard culture conditions and its extracellular and cell-surface activity can be detected even in non-stimulated, early post-confluent cultures.[10,54] Therefore, measurement of TG2 activity in our experimental setup does not necessarily require fully differentiated enterocyte-like cells. Importantly, to account for potential differences in differentiation status, experiments assessing gene and protein expression were performed at later time points (10 to 12 days post confluence), while early post-confluent cultures were used specifically for viability and extracellular activity measurements.

Recent reports suggested that ACN can directly bind to gliadin peptides.[21–23,26,55,56] However, in other studies, it has been observed that ACN can interact with enzymes, thereby modulating their activity. For digestive enzymes, this was shown by enzyme kinetics, affinity ultrafiltration, spectroscopy and *in silico* analyses.[57,58] Xie *et al.* found that ACN directly bound and inhibited oxidoreductive enzymes such as xanthine oxidase.[59] This raised the question whether our findings are based on the binding of ACN to the peptides or on a direct interaction with the enzyme. The investigation of crosslinking using the TG2 substrate 5BP instead of gliadin peptides with and without calcium addition initially suggests that the observed reduction in crosslinking is not necessarily caused by a specific interaction with gliadin (Fig. 1C).

To examine the question in greater depth, STD-NMR experiments were performed which provide insights into the location and intensity of the binding. Simultaneous incubation significantly altered the ^{1}H NMR spectrum of C3G and D3G, which indicated an interaction with TG2, mainly by the glucoside residue (Fig. 3). To further analyze the functional relevance of this interaction, we performed *in silico* docking experiments. We found 5 similar binding sites for C3G and D3G with moderate (−4 to −8 kcal mol^{-1}) and high (>−8 kcal mol^{-1}) affinity scores. Even though there was no proximity to the active center, we identified two binding sites with contact to regions within the 3D structure of TG2 that are essential for calcium binding. Especially the binding site C2 showed a high affinity and the contact residues have been described as calcium binding sites before.[31,32] Calcium binding is essential for TG2 function since it causes a change in the conformation of the enzyme which is required for its transamidase function. High concentrations of free calcium therefore activate the crosslinking activity.[37,60] Based on these findings, we performed enzyme activity assays and observed that the inhibitory effect of D3G was more prominent at higher calcium concentrations (Fig. 4).

Since ACN are also known to have anti-inflammatory properties, we next focused on the influence of C3G and D3G on CD-associated inflammation. Therefore, we used a cell culture model of CD-inflammation by stimulating Caco-2 cells with the main Th1-cytokines IFN-γ and TNF-α. Under non-inflammatory conditions, C3G and D3G did not affect cell viability. Simultaneous administration of C3G and IFN-γ or TNF-α significantly improved cell viability compared to the treatment with cytokines only (Fig. 5A). Addition of D3G had a positive effect on the cell viability compared to treatment with IFN-γ, but not with TNF-α (Fig. 5B). Here, cells were used at an early differentiation time point (4 to 7 days after confluence), as cell viability assays reflect fundamental cellular processes that are already established in early post-confluent monolayers. Accordingly, early post-confluent Caco-2 cultures represent a suitable and widely used model for viability measurements.[61–66] Nevertheless, it should be noted that the findings cannot be directly extrapolated to fully differentiated intestinal epithelium.

As a next step, we investigated whether ACN would also attenuate cytokine-mediated elevation of TG2 expression in Caco-2 cells. Here, we demonstrated a significant increase in TG2 mRNA and protein levels after stimulation with IFN-γ, whereas TNF-α did not have any effect. When D3G was simultaneously incubated with IFN-γ, the TG2 mRNA was significantly reduced. Although D3G did not significantly affect TG2 protein levels, for C3G a trend toward decreased protein abundance with borderline significance (p = 0.056) was noted. However, this requires confirmation in studies with larger sample sizes.

We hypothesized that a molecular interaction between the ACN and the cytokines and their corresponding receptors were the mechanism behind these effects. To explore potential interactions, we performed *in silico* docking analyses. For the IFN-γ receptor complex and C3G or D3G, we identified three binding sites (C1, C2 and C4) with high affinity and potential functional significance (Fig. 7A). The contact residues of all binding sites included I149, K167 and N174 of IFN-γR1 and D164 and T168 of IFN-γR2, which have been described by Walter *et al.* and Mendoza *et al.* as being crucial for the assembly and stability of the IFN-γ receptor complex. Furthermore, binding sites C1 and C2 had multiple contact residues within regions of IFN-γ that are essential for the interaction between the cytokine and IFN-γR1 (amino acids 1–42).[34,35] The docking experiments between the TNF-α receptor complex and C3G or D3G revealed four binding sites with moderate to high affinity and potential functional significance (Fig. 7B). The contact residues of those binding sites included regions (amino acids 30–36 and 140–147) that have been shown by Van Ostade *et al.* and Idriss *et al.* to be critical for TNF-α receptor binding and the resulting cytotoxic effects.[67–69] Furthermore, Uversky *et al.* demonstrated that these regions are essential for receptor interaction and signal transduction.[70] This agreement may suggest that the predicted binding sites could potentially

affect cytokine receptor interactions relevant to inflammatory signalling.

Our findings are in line with previous reports where Caco-2 cells were shown to express IFN-γ and TNF-α receptors. In particular, Chavez *et al.* demonstrated that IFN-γ responsiveness develops during Caco-2 differentiation and Wang *et al.* described that TNF-αR2 plays a role in inflammation-associated loss of epithelial barrier integrity.[71,72] In addition, a molecular interaction of C3G with IL17 and its receptor IL17-RA that attenuated IL-17-mediated inflammation was described by Liu *et al.*[73] Finally, *in silico* analyses and functional data have shown that ACN reduced programmed cell death protein-1 (PD-1) and programmed cell death protein ligand-1 (PD-L1)-signaling by direct molecular interaction.[42,74]

Conclusion

Our data suggest that C3G and D3G inhibit TG2 activity in a recombinant system, while effects on extracellular TG2 activity in a Caco-2 model were limited and should be further addressed in future studies. Moreover, the initial results obtained by molecular docking analysis suggest that a direct molecular interaction is involved in a possible attenuation of the inflammatory effects mediated by IFN-γ and TNF-α. The administration of ACN may also be accompanied by other beneficial effects such as a reduction in oxidative stress and an improved intestinal epithelial barrier integrity.[26,40,75–77] Furthermore, D3G may modulate TG2 expression at the mRNA level, although this was not confirmed at the protein level. These findings support the potential of ACN as natural modulators of TG2, the key enzyme in the context of CD pathology. However, further studies are needed to confirm the relevance of ACN as a TG2 inhibitor in humans.

Author contributions

Andrea Diers: investigation (lead), data curation (lead), formal analysis (lead), writing – original draft preparation (lead). Silvia Rudloff: conceptualization (supporting), methodology (supporting), supervision (supporting), writing – review and editing (supporting). Heike Hausmann: methodology (supporting), formal analysis (supporting), writing – review and editing (supporting). Anika E. Wagner: conceptualization (supporting), methodology (supporting), writing – review and editing (supporting). Sebastian Stricker: conceptualization (lead), methodology (lead), supervision (lead), writing – review and editing (lead). All authors have read and agreed to the published version of this manuscript.

Conflicts of interest

There are no conflicts of interest to declare.

Data availability

The data presented in this study are available on request from the corresponding author.

Supplementary information (SI) is available. See DOI: https://doi.org/10.1039/d6fo00704j.

Acknowledgements

We thank Dr Johannes Herrmann, Statistical Consulting Services, Giessen, Germany for statistical advice. We are grateful to Larissa Thiessen, Nadine Böcher, Stephanie Schmitt and Cordula Becker for their excellent technical assistance.

References

1 L. M. Sollid, G. Markussen, J. Ek, H. Gjerde, F. Vartdal and E. Thorsby, Evidence for a primary association of celiac disease to a particular HLA-DQ alpha/beta heterodimer, *J. Exp. Med.*, 1989, **169**, 345–350.
2 S. Nardecchia, R. Auricchio, V. Discepolo and R. Troncone, Extra-Intestinal Manifestations of Coeliac Disease in Children: Clinical Features and Mechanisms, *Front. Pediatr.*, 2019, **7**, 56.
3 B. Lebwohl, P. H. R. Green, J. Söderling, B. Roelstraete and J. F. Ludvigsson, Association Between Celiac Disease and Mortality Risk in a Swedish Population, *J. Am. Med. Assoc.*, 2020, **323**, 1277–1285.
4 B. Lebwohl, D. S. Sanders and P. H. R. Green, Coeliac disease, *Lancet*, 2018, **391**, 70–81.
5 O. Molberg, S. N. Mcadam, R. Körner, H. Quarsten, C. Kristiansen, L. Madsen, L. Fugger, H. Scott, O. Norén, P. Roepstorff, K. E. Lundin, H. Sjöström and L. M. Sollid, Tissue transglutaminase selectively modifies gliadin peptides that are recognized by gut-derived T cells in celiac disease, *Nat. Med.*, 1998, **4**, 713–717.
6 H. Arentz-Hansen, R. Körner, O. Molberg, H. Quarsten, W. Vader, Y. M. Kooy, K. E. Lundin, F. Koning, P. Roepstorff, L. M. Sollid and S. N. McAdam, The intestinal T cell response to alpha-gliadin in adult celiac disease is focused on a single deamidated glutamine targeted by tissue transglutaminase, *J. Exp. Med.*, 2000, **191**, 603–612.
7 L. Shan, Ø. Molberg, I. Parrot, F. Hausch, F. Filiz, G. M. Gray, L. M. Sollid and C. Khosla, Structural basis for gluten intolerance in celiac sprue, *Science*, 2002, **297**, 2275–2279.
8 T. Rauhavirta, S.-W. Qiao, Z. Jiang, E. Myrsky, J. Loponen, I. R. Korponay-Szabó, H. Salovaara, J. A. Garcia-Horsman, J. Venäläinen, P. T. Männistö, R. Collighan, A. Mongeot, M. Griffin, M. Mäki, K. Kaukinen and K. Lindfors, Epithelial transport and deamidation of gliadin peptides: a role for coeliac disease patient immunoglobulin A, *Clin. Exp. Immunol.*, 2011, **164**, 127–136.
9 C. Lebreton, S. Ménard, J. Abed, I. C. Moura, R. Coppo, C. Dugave, R. C. Monteiro, A. Fricot, M. G. Traore,

M. Griffin, C. Cellier, G. Malamut, N. Cerf-Bensussan and M. Heyman, Interactions among secretory immunoglobulin A, CD71, and transglutaminase-2 affect permeability of intestinal epithelial cells to gliadin peptides, *Gastroenterology*, 2012, **143**, 698–707.

10 S. Stricker, J. de Laffolie, K.-P. Zimmer and S. Rudloff, Inhibition of Transglutaminase 2 as a Therapeutic Strategy in Celiac Disease-In Vitro Studies in Intestinal Cells and Duodenal Biopsies, *Int. J. Mol. Sci.*, 2023, **24**, 4795.

11 S. F. Amundsen, J. Stamnaes, K. E. A. Lundin and L. M. Sollid, Expression of transglutaminase 2 in human gut epithelial cells: Implications for coeliac disease, *PLoS One*, 2023, **18**, e0287662.

12 M. T. Meling, L. Kleppa, H. A. Besser, C. Khosla, M. F. du Pré and L. M. Sollid, Enterocyte-Derived and Catalytically Active Transglutaminase 2 in the Gut Lumen of Mice: Implications for Celiac Disease, *Gastroenterology*, 2024, **167**, 1026–1028.

13 G. Ferretti, T. Bacchetti, S. Masciangelo and L. Saturni, Celiac disease, inflammation and oxidative damage: a nutrigenetic approach, *Nutrients*, 2012, **4**, 243–257.

14 S. R. Bozorg, A. R. Lee, K. Mårild and J. A. Murray, The Economic Iceberg of Celiac Disease: More Than the Cost of Gluten-Free Food, *Gastroenterology*, 2024, **167**, 172–182.

15 B. Bokemeyer, L. Serdani-Neuhaus, J. Sünwoldt, C. Dünweber, S. Schnaidt and D. Schuppan, Burden of coeliac disease in Germany: real-world insights from a large retrospective health insurance claims database analysis, *Therap. Adv. Gastroenterol.*, 2025, **18**, 17562848251314803.

16 G. Czaja-Bulsa and M. Bulsa, Adherence to Gluten-Free Diet in Children with Celiac Disease, *Nutrients*, 2018, **10**, 1424.

17 A. Myléus, N. R. Reilly and P. H. R. Green, Rate, Risk Factors, and Outcomes of Nonadherence in Pediatric Patients With Celiac Disease: A Systematic Review, *Clin. Gastroenterol. Hepatol.*, 2020, **18**, 562–573.

18 S. Kuntz, C. Kunz, J. Herrmann, C. H. Borsch, G. Abel, B. Fröhling, H. Dietrich and S. Rudloff, Anthocyanins from fruit juices improve the antioxidant status of healthy young female volunteers without affecting anti-inflammatory parameters: results from the randomised, double-blind, placebo-controlled, cross-over ANTHONIA (ANTHOcyanins in Nutrition Investigation Alliance) study, *Br. J. Nutr.*, 2014, **112**, 925–936.

19 S. Kuntz, H. Asseburg, S. Dold, A. Römpp, B. Fröhling, C. Kunz and S. Rudloff, Inhibition of low-grade inflammation by anthocyanins from grape extract in an in vitro epithelial-endothelial co-culture model, *Food Funct.*, 2015, **6**, 1136–1149.

20 S. Kuntz, C. Kunz, E. Domann, N. Würdemann, F. Unger, A. Römpp and S. Rudloff, Inhibition of Low-Grade Inflammation by Anthocyanins after Microbial Fermentation in Vitro, *Nutrients*, 2016, **8**, 411.

21 P. Mazzaracchio, S. Tozzi, C. Boga, L. Forlani, P. G. Pifferi and G. Barbiroli, Interaction between gliadins and anthocyan derivatives, *Food Chem.*, 2011, **129**, 1100–1107.

22 P. Taddei, N. Zanna and S. Tozzi, Raman characterization of the interactions between gliadins and anthocyanins, *J. Raman Spectrosc.*, 2013, **44**, 1435–1439.

23 Z. Guo, Y. Huang, J. Huang, S. Li, Z. Zhu, Q. Deng and S. Cheng, Formation of protein-anthocyanin complex induced by grape skin extracts interacting with wheat gliadins: Multi-spectroscopy and molecular docking analysis, *Food Chem.*, 2022, **385**, 132702.

24 R. Mattioli, A. Francioso, L. Mosca and P. Silva, Anthocyanins: A Comprehensive Review of Their Chemical Properties and Health Effects on Cardiovascular and Neurodegenerative Diseases, *Molecules*, 2020, **25**, 3809.

25 D. Ferrari, F. Cimino, D. Fratantonio, M. S. Molonia, R. Bashllari, R. Busà, A. Saija and A. Speciale, Cyanidin-3-O-Glucoside Modulates the In Vitro Inflammatory Crosstalk between Intestinal Epithelial and Endothelial Cells, *Mediators Inflammation*, 2017, **2017**, 3454023.

26 Á. Klusóczki, B. Oláh, D. Hosszú, F. Fenyvesi, J. Remenyik, J. Homoki, A. Gyöngyösi, I. Bácskay and J. Váradi, Effectiveness of Anthocyanin-Rich Sour Cherry Extract on Gliadin-Induced Caco-2 Barrier Damage, *Nutrients*, 2023, **15**, 4022.

27 S. Piazza, F. Colombo, C. Bani, M. Fumagalli, O. Vincentini, E. Sangiovanni, G. Martinelli, S. Biella, M. Silano, P. Restani, M. Dell'Agli and C. Di Lorenzo, Evaluation of the Potential Anti-Inflammatory Activity of Black Rice in the Framework of Celiac Disease, *Foods*, 2022, **12**, 63.

28 B. Meyer and T. Peters, NMR spectroscopy techniques for screening and identifying ligand binding to protein receptors, *Angew. Chem., Int. Ed.*, 2003, **42**, 864–890.

29 Y. Liu, X. Yang, J. Gan, S. Chen, Z.-X. Xiao and Y. Cao, CB-Dock2: improved protein-ligand blind docking by integrating cavity detection, docking and homologous template fitting, *Nucleic Acids Res.*, 2022, **50**, W159–W164.

30 N. Yanamala, A. Dutta, B. Beck, B. van Fleet, K. Hay, A. Yazbak, R. Ishima, A. Doemling and J. Klein-Seetharaman, NMR-based screening of membrane protein ligands, *Chem. Biol. Drug Des.*, 2010, **75**, 237–256.

31 R. Király, E. Csosz, T. Kurtán, S. Antus, K. Szigeti, Z. Simon-Vecsei, I. R. Korponay-Szabó, Z. Keresztessy and L. Fésüs, Functional significance of five noncanonical Ca2+-binding sites of human transglutaminase 2 characterized by site-directed mutagenesis, *FEBS J.*, 2009, **276**, 7083–7096.

32 R. Király, M. Demény and L. Fésüs, Protein transamidation by transglutaminase 2 in cells: a disputed Ca2+-dependent action of a multifunctional protein, *FEBS J.*, 2011, **278**, 4717–4739.

33 E. M. Jeong, K. B. Lee, G. E. Kim, C. M. Kim, J.-H. Lee, H.-J. Kim, J.-W. Shin, M.-A. Kwon, H. H. Park and I.-G. Kim, Competitive Binding of Magnesium to Calcium Binding Sites Reciprocally Regulates Transamidase and GTP Hydrolysis Activity of Transglutaminase 2, *Int. J. Mol. Sci.*, 2020, **21**, 791.

34 M. R. Walter, W. T. Windsor, T. L. Nagabhushan, D. J. Lundell, C. A. Lunn, P. J. Zauodny and S. K. Narula,

Crystal structure of a complex between interferon-gamma and its soluble high-affinity receptor, *Nature*, 1995, **376**, 230–235.

35 J. L. Mendoza, N. K. Escalante, K. M. Jude, J. Sotolongo Bellon, L. Su, T. M. Horton, N. Tsutsumi, S. J. Berardinelli, R. S. Haltiwanger, J. Piehler, E. G. Engleman and K. C. Garcia, Structure of the IFNγ receptor complex guides design of biased agonists, *Nature*, 2019, **567**, 56–60.

36 D. Schuppan, M. Mäki, K. E. A. Lundin, J. Isola, T. Friesing-Sosnik, J. Taavela, A. Popp, J. Koskenpato, J. Langhorst, Ø. Hovde, M.-L. Lähdeaho, S. Fusco, M. Schumann, H. P. Török, J. Kupcinskas, Y. Zopf, A. W. Lohse, M. Scheinin, K. Kull, L. Biedermann, V. Byrnes, A. Stallmach, J. Jahnsen, J. Zeitz, R. Mohrbacher, R. Greinwald and CEC-3 Trial Group, A Randomized Trial of a Transglutaminase 2 Inhibitor for Celiac Disease, *N. Engl. J. Med.*, 2021, **385**, 35–45.

37 Z. Yao, Y. Fan, L. Lin, R. E. Kellems and Y. Xia, Tissue transglutaminase: a multifunctional and multisite regulator in health and disease, *Physiol. Rev.*, 2024, **104**, 281–325.

38 J. Cvorovic, F. Tramer, M. Granzotto, L. Candussio, G. Decorti and S. Passamonti, Oxidative stress-based cytotoxicity of delphinidin and cyanidin in colon cancer cells, *Arch. Biochem. Biophys.*, 2010, **501**, 151–157.

39 S. Kuntz, S. Rudloff, H. Asseburg, C. Borsch, B. Fröhling, F. Unger, S. Dold, B. Spengler, A. Römpp and C. Kunz, Uptake and bioavailability of anthocyanins and phenolic acids from grape/blueberry juice and smoothie in vitro and in vivo, *Br. J. Nutr.*, 2015, **113**, 1044–1055.

40 E. Cremonini, A. Mastaloudis, S. N. Hester, S. V. Verstraeten, M. Anderson, S. M. Wood, A. L. Waterhouse, C. G. Fraga and P. I. Oteiza, Anthocyanins inhibit tumor necrosis alpha-induced loss of Caco-2 cell barrier integrity, *Food Funct.*, 2017, **8**, 2915–2923.

41 I. M. A. Ernst, A. E. Wagner, P. Huebbe and G. Rimbach, Cyanidin does not affect sulforaphane-mediated Nrf2 induction in cultured human keratinocytes, *Br. J. Nutr.*, 2012, **107**, 360–363.

42 C. Mazewski, M. S. Kim and E. Gonzalez de Mejia, Anthocyanins, delphinidin-3-O-glucoside and cyanidin-3-O-glucoside, inhibit immune checkpoints in human colorectal cancer cells in vitro and in silico, *Sci. Rep.*, 2019, **9**, 11560.

43 D. B. Haytowitz, X. Wu and S. Bhagwat, *USDA Database for the Flavonoid Content of Selected Foods, Release 3.3*, U.S. Department of Agriculture, Agricultural Research Service.

44 D. M. Mudie, G. L. Amidon and G. E. Amidon, Physiological parameters for oral delivery and in vitro testing, *Mol. Pharm.*, 2010, **7**, 1388–1405.

45 D. Mueller, K. Jung, M. Winter, D. Rogoll, R. Melcher, U. Kulozik, K. Schwarz and E. Richling, Encapsulation of anthocyanins from bilberries – Effects on bioavailability and intestinal accessibility in humans, *Food Chem.*, 2018, **248**, 217–224.

46 S. Chen, R. Einspanier and J. Schoen, Transepithelial electrical resistance (TEER): a functional parameter to monitor the quality of oviduct epithelial cells cultured on filter supports, *Histochem. Cell Biol.*, 2015, **144**, 509–515.

47 M. J. Briske-Anderson, J. W. Finley and S. M. Newman, The influence of culture time and passage number on the morphological and physiological development of Caco-2 cells, *Proc. Soc. Exp. Biol. Med.*, 1997, **214**, 248–257.

48 I. Legen, M. Salobir and J. Kerč, Comparison of different intestinal epithelia as models for absorption enhancement studies, *Int. J. Pharm.*, 2005, **291**, 183–188.

49 H. Kawaguchi, Y. Akazawa, Y. Watanabe and Y. Takakura, Permeability modulation of human intestinal Caco-2 cell monolayers by interferons, *Eur. J. Pharm. Biopharm.*, 2005, **59**, 45–50.

50 A. Olejnik, R. Marecik, M. Skrzypczak, K. Czaczyk and W. Włodzimierz, Application of rapid Caco-2 cell culture system in the studies on the bacterial adhesion and transepithelial transport, *Pol. J. Food Nutr. Sci.*, 2008, **58**, 365–371.

51 A. L. Kauffman, A. V. Gyurdieva, J. R. Mabus, C. Ferguson, Z. Yan and P. J. Hornby, Alternative functional in vitro models of human intestinal epithelia, *Front. Pharmacol.*, 2013, **4**, 79.

52 T. Tsushima, T. Ohkubo, K. Onoyama, M. Linder and K. Takahashi, Lysophosphatidylserine form DHA maybe the most effective as substrate for brain DHA accretion, *Biocatal. Agric. Biotechnol.*, 2014, **3**, 303–309.

53 R. Wongwanakul, S. Aueviriyavit, T. Furihata, P. Gonil, W. Sajomsang, R. Maniratanachote and S. Jianmongkol, Quaternization of high molecular weight chitosan for increasing intestinal drug absorption using Caco-2 cells as an in vitro intestinal model, *Sci. Rep.*, 2023, **13**, 7904.

54 M. Bayardo, F. Punzi, C. Bondar, N. Chopita and F. Chirdo, Transglutaminase 2 expression is enhanced synergistically by interferon-γ and tumour necrosis factor-α in human small intestine, *Clin. Exp. Immunol.*, 2012, **168**, 95–104.

55 S. Tozzi, N. Zanna and P. Taddei, Study on the interaction between gliadins and a coumarin as molecular model system of the gliadins-anthocyanidins complexes, *Food Chem.*, 2013, **141**, 3586–3597.

56 C. B. Van Buiten and R. J. Elias, Gliadin Sequestration as a Novel Therapy for Celiac Disease: A Prospective Application for Polyphenols, *Int. J. Mol. Sci.*, 2021, **22**, 595.

57 S. Akkarachiyasit, P. Charoenlertkul, S. Yibchok-Anun and S. Adisakwattana, Inhibitory activities of cyanidin and its glycosides and synergistic effect with acarbose against intestinal α-glucosidase and pancreatic α-amylase, *Int. J. Mol. Sci.*, 2010, **11**, 3387–3396.

58 Y. Wang, L. Chen, H. Liu, J. Xie, W. Yin, Z. Xu, H. Ma, W. Wu, M. Zheng, M. Liu and J. Liu, Characterization of the synergistic inhibitory effect of cyanidin-3-O-glucoside and catechin on pancreatic lipase, *Food Chem.*, 2023, **404**, 134672.

59 J. Xie, H. Cui, Y. Xu, L. Xie and W. Chen, Delphinidin-3-O-sambubioside: a novel xanthine oxidase inhibitor identified from natural anthocyanins, *Food Qual. Saf.*, 2021, **5**, fyaa038.

60 R. Király, M.átéÁ. Demény and L. Fésüs, Protein transamidation by transglutaminase 2 in cells: a disputed Ca2+-dependent action of a multifunctional protein, *FEBS J.*, 2011, **278**, 4717–4739.
61 S. C. Forester and A. L. Waterhouse, Gut Metabolites of Anthocyanins, Gallic Acid, 3-O-Methylgallic Acid, and 2,4,6-Trihydroxybenzaldehyde, Inhibit Cell Proliferation of Caco-2 Cells, *J. Agric. Food Chem.*, 2010, **58**, 5320–5327.
62 M. Schantz, C. Mohn, M. Baum and E. Richling, Antioxidative efficiency of an anthocyanin rich bilberry extract in the human colon tumor cell lines Caco-2 and HT-29, *J. Berry Res.*, 2010, **1**, 25–33.
63 H. Jung, H. J. Lee, H. Cho and K. T. Hwang, Anti-Inflammatory Activities of Rubus Fruit Anthocyanins in Inflamed Human Intestinal Epithelial Cells, *J. Food Biochem.*, 2015, **39**, 300–309.
64 A. Nowak, M. Zakłos-Szyda, D. Żyżelewicz, A. Koszucka and I. Motyl, Acrylamide Decreases Cell Viability, and Provides Oxidative Stress, DNA Damage, and Apoptosis in Human Colon Adenocarcinoma Cell Line Caco-2, *Molecules*, 2020, **25**, 368.
65 M. Zakłos-Szyda, N. Pietrzyk, A. Kowalska-Baron, A. Nowak, K. Chałaśkiewicz, M. Ratajewski, G. Budryn and M. Koziołkiewicz, Phenolics-Rich Extracts of Dietary Plants as Regulators of Fructose Uptake in Caco-2 Cells via GLUT5 Involvement, *Molecules*, 2021, **26**, 4745.
66 H. A. S. N. Abeysiri, K. T. Dilrukshi, S. A. Kulasooriya and P. M. Manage, In Vitro Assay for Determining Cyanotoxin Using Cell Line Method: Hepatotoxicity (Cell Lines—HepG2, Caco-2, and V79), in *Protocols for Cyanobacteria Sampling and Detection of Cyanotoxin*, ed. N. Thajuddin, A. Sankara narayanan and D. Dhanasekaran, Springer Nature, Singapore, 2023, pp. 253–257.
67 X. Van Ostade, P. Vandenabeele, B. Everaerdt, H. Loetscher, R. Gentz, M. Brockhaus, W. Lesslauer, J. Tavernier, P. Brouckaert and W. Fiers, Human TNF mutants with selective activity on the p55 receptor, *Nature*, 1993, **361**, 266–269.
68 X. Van Ostade, P. Vandenabeele, J. Tavernier and W. Fiers, Human tumor necrosis factor mutants with preferential binding to and activity on either the R55 or R75 receptor, *Eur. J. Biochem.*, 1994, **220**, 771–779.
69 H. T. Idriss and J. H. Naismith, TNF alpha and the TNF receptor superfamily: structure-function relationship(s), *Microsc. Res. Tech.*, 2000, **50**, 184–195.
70 V. N. Uversky, N. A. El-Baky, E. M. El-Fakharany, A. Sabry, E. H. Mattar, A. V. Uversky and E. M. Redwan, Functionality of intrinsic disorder in tumor necrosis factor-α and its receptors, *FEBS J.*, 2017, **284**, 3589–3618.
71 A. M. Chavez, M. J. Morin, N. Unno, M. P. Fink and R. A. Hodin, Acquired interferon gamma responsiveness during Caco-2 cell differentiation: effects on iNOS gene expression, *Gut*, 1999, **44**, 659–665.
72 F. Wang, B. T. Schwarz, W. V. Graham, Y. Wang, L. Su, D. R. Clayburgh, C. Abraham and J. R. Turner, IFN-gamma-induced TNFR2 expression is required for TNF-dependent intestinal epithelial barrier dysfunction, *Gastroenterology*, 2006, **131**, 1153–1163.
73 C. Liu, L. Zhu, K. Fukuda, S. Ouyang, X. Chen, C. Wang, C. Zhang, B. Martin, C. Gu, L. Qin, S. Rachakonda, M. Aronica, J. Qin and X. Li, The flavonoid cyanidin blocks binding of the cytokine interleukin-17A to the IL-17RA subunit to alleviate inflammation in vivo, *Sci. Signal.*, 2017, **10**, eaaf8823.
74 G. R. Sartori, A. de O. Albuquerque, A. H. Santos-Costa, L. M. Andrade, D. da S. Almeida, E. M. Gaieta, J. V. Sampaio, V. T. de M. L. Albuquerque and J. H. Martins Da Silva, In silico mapping of the dynamic interactions and structure-activity relationship of flavonoid compounds against the immune checkpoint programmed-cell death 1 pathway, *Front. Drug Discov.*, 2022, **2**, 1032587.
75 M. Dueñas, I. Muñoz-González, C. Cueva, A. Jiménez-Girón, F. Sánchez-Patán, C. Santos-Buelga, M. V. Moreno-Arribas and B. Bartolomé, A survey of modulation of gut microbiota by dietary polyphenols, *BioMed Res. Int.*, 2015, **2015**, 850902.
76 R. Yin, H.-C. Kuo, R. Hudlikar, D. Sargsyan, S. Li, L. Wang, R. Wu and A.-N. Kong, Gut microbiota, dietary phytochemicals and benefits to human health, *Curr. Pharmacol. Rep.*, 2019, **5**, 332–344.
77 P. Tu, X. Zheng, H. Niu, Z. Chen, X. Wang, L. Wu and Q. Tang, Characterizing the Gut Microbial Metabolic Profile of Mice with the Administration of Berry-Derived Cyanidin-3-Glucoside, *Metabolites*, 2023, **13**, 818.